Journal of Maps

ISSN: (Print) (Online) Journal homepage: www.tandfonline.com/journals/tjom20

Areas simultaneously susceptible and (dis-)connected to debris flows in the Dolomites (Italy): regional-scale application of a novel data-driven approach

Felix Pitscheider, Stefan Steger, Marco Cavalli, Francesco Comiti & Vittoria Scorpio

To cite this article: Felix Pitscheider, Stefan Steger, Marco Cavalli, Francesco Comiti & Vittoria Scorpio (2024) Areas simultaneously susceptible and (dis-)connected to debris flows in the Dolomites (Italy): regional-scale application of a novel data-driven approach, Journal of Maps, 20:1, 1-14, DOI: 10.1080/17445647.2024.2307549

To link to this article: https://doi.org/10.1080/17445647.2024.2307549

JOURNAL OF MAPS
2024, VOL. 20, NO. 1, 2307549
https://doi.org/10.1080/17445647.2024.2307549

SCIENCE

OPEN ACCESS Check for updates

Areas simultaneously susceptible and (dis-)connected to debris flows in the Dolomites (Italy): regional-scale application of a novel data-driven approach

Felix Pitscheider[a], Stefan Steger[b]*, Marco Cavalli[c], Francesco Comiti[a]** and Vittoria Scorpio[d]

[a]Faculty of Agricultural, Environmental and Food Sciences, Free University of Bozen-Bolzano, Bolzano, Italy; [b]Eurac Research, Center for Climate Change and Transformation, Bolzano, Italy; [c]Research Institute for Geo-hydrological Protection, National Research Council (CNR IRPI), Padova, Italy; [d]Department of Chemical and Geological Sciences, University of Modena and Reggio Emilia, Modena, Italy

ABSTRACT

In mountain regions, the impact of areas on the sediment conveyance can not only be described by their susceptibility to debris flow release, but also by their structural connectivity to the rivers. This generates the need to combine susceptibility and connectivity for accurate analyses of sediment transport. Our study exploits an approach developed by [Steger, er al. 2022; https://doi.org/10.1002/esp.5421] and upscales it to the South Tyrolean Dolomites region. The approach comprised the modeling of debris flow release susceptibility using an interpretable machine learning algorithm, the training of a logistic regression model, and the combination of the resultant classified maps to create a joint susceptibility-connectivity map. The results show the quantitative thresholds for the susceptibility probability and the Index of Connectivity (IC) that allow to discriminate between susceptible and not susceptible, as well as connected and disconnected areas, which are represented via a variety of maps.

Key policy highlights

- The upscaling of a debris flow susceptibility-connectivity mapping model was successfully carried out with only moderate adjustments needed.
- The model is an effective and resource-efficient tool for evaluating potentially threatening areas and can help focus mitigation efforts.
- Compared to the western South Tyrolean Dolomites, the areas in the east are more susceptible to debris flows which are simultaneously connected to the channel network.

ARTICLE HISTORY
Received 19 January 2023
Revised 9 January 2024
Accepted 12 January 2024

KEYWORDS
Sediment connectivity; debris flow susceptibility; regional-scale analysis; hazard mapping; hillslope-channel coupling; GIS

1. Introduction

Debris flows are amongst the most common and impacting natural hazards in mountain areas, and these processes represent particularly important mechanisms for sediment supply and transport in mountain catchments (Brardinoni et al., 2015; Cislaghi & Bischetti, 2019; Schopper et al., 2019; Schuerch et al., 2006; Stoffel et al., 2016). Risk mitigation for debris flows greatly benefit from the investigation of past events, especially in terms of the initiation sites where the sediments were initially mobilized, and in regarding their downslope path and run-out distance.

The run-out distance of debris flows is highly linked to the concept of sediment connectivity when analyzing sediment transfer at the catchment scale. The expression 'sediment connectivity' refers to the degree to which a system controls the transfer of sediment through itself (Bracken et al., 2015; Heckmann et al., 2018; Wohl et al., 2019). The sediment connectivity concept can be used to explain the continuity of sediment transfer from source areas to downstream areas (Cavalli et al., 2019). It represents an emerging system property of geomorphic systems (Wohl et al., 2019) that can help decipher relationships between hillslopes and channels (lateral connectivity) or along channels (longitudinal connectivity) (Bracken et al., 2015; Brierley et al., 2006; Fryirs et al., 2007). Sediment connectivity can be investigated by considering its structural and functional aspects (*sensu* Wainwright et al., 2011). In particular, the structural connectivity describes the extent to which landscape units are contiguous or physically linked to one another (Cavalli et al., 2017; Tischendorf & Fahrig, 2000). The functional connectivity relates to the dynamics of geomorphic and

CONTACT Vittoria Scorpio vittoria.scorpio@unimore.it Department of Chemical and Geological Sciences, University of Modena and Reggio Emilia, via Campi 103, 41125 Modena, Italy
*Present address: GeoSphere Austria, Vienna, Austria
**Dept. Land, Environment, Agriculture and Forestry, University of Padova, Padova, Italy
Supplemental data for this article can be accessed online at https://doi.org/10.1080/17445647.2024.2307549.

hydrologic processes within a catchment (Bracken et al., 2013; Wainwright et al., 2011).

GIS-based approaches that focus on the characterization and mapping of structurally connected terrain do usually not consider that a laterally connected area is not necessarily prone to release the phenomena under investigation, such as flow-type or slide-type landslides. The identification of areas most relevant to provide mass movement material to a downslope channel system, therefore, requires accounting for both, sediment connectivity and mass movement release susceptibility (Steger et al., 2022).

The data-driven mapping of areas susceptible to different types of landslides has gained momentum during the last decades with hundreds of published case studies each year (Lima et al., 2022; Reichenbach et al., 2018). Data-driven landslide susceptibility analyses formally focus on the spatial domain to map areas where landslides are more and less likely to occur given a set of geo-environmental information. This is usually done by using a statistical or machine learning classifier that links spatial data on past landslide occurrence (i.e. landslide inventory) and non-occurrence (i.e. landslide absences) with spatial features acting as proxies for the prevalent morphological, hydro-geological and land cover conditions (Reichenbach et al., 2018; Steger & Kofler, 2019). When assessing landslide susceptibility, it is important to highlight whether the respective model refers to the process source zone or to the traveling or deposit zones. This is particularly true for mass movements with potentially long travel distances, such as debris flows. In fact, debris flow release susceptibility models are built upon landslide data representing debris flow source zones and therefore identify areas where a debris flow is more likely to be initiated (Goetz et al., 2021; Heckmann et al., 2014).

Early connectivity mapping was mainly performed by utilizing aerial photos and field data to study mass movements (e.g. Brardinoni & Hassan, 2006; Hooke, 2003; Schrott et al., 2003). With the advent of high-resolution topographic data, new models to assess and map sediment connectivity have been developed. Walling and Zhang (2004) were among the first to analyze sediment connectivity based on spatial datasets. Borselli et al. (2008) developed an index of connectivity, which was further adapted to map structural connectivity in mountain basins by Cavalli et al. (2013).

Despite the relatively high number of published research in the fields of debris flow susceptibility and sediment connectivity analyses, to our knowledge, until recently no maps have been published to identify areas that are simultaneously susceptible to debris flow initiation and structurally connected to the main channel network. Recently, Spiekermann et al. (2022) coupled logistic regression-based shallow landslide susceptibility and connectivity predictions in a modular way for an area in New Zealand. Steger et al. (2022) focused on debris flow release susceptibility and connectivity in three river catchments of South Tyrol (Northern Italy), namely the Stolla (40 km²), Pfitsch (140 km²), and Sulden (160 km²) catchments. The present study takes advantage of the data-driven model proposed by Steger et al. (2022) and aims at upscaling it to a regional scale, i.e. to the portion of the 'Dolomites' located in South Tyrol, an area of about 1,160 km².

2. Study area

The so-called 'Dolomites' lie in the south-eastern sector of the Alps (Figure 1). The study area falls within the Province of Bolzano-Bozen (Italy) and is characterized by elevations ranging from 277 to 3173 m a.s.l..

The Dolomites have a continental climate with significant daily temperature variations. Annual precipitation ranges from 500 to 1500 mm and is mostly in the form of intense, convective rainfall events during summer (Crespi et al., 2021). From a geological perspective, Dolomites are composed of a Hercinian crystalline basement (phyllites, micaschists and paragneisses) covered by Permo-mesozoic sedimentary successions in fluvial to shallow marine environment (sandstones and marly limestones) and by dolomites and limestones deposited in the Triassic. Permian volcanic rocks outcrop in the south-western sector of the study area (Figure 1(B)).

During the Quaternary, the landscape was shaped by glaciers, which left landforms and extensive till and fluvioglacial deposits. These deposits have been promptly eroded by colluvial and alluvial processes since the early Holocene (Stingl & Mair, 2005).

This study encompasses the eleven river catchments situated in the South Tyrolean Dolomites (Figure 1(A); Table 1). The studied catchments were derived by determining the drainage areas of the rivers at their confluences with a larger water body. For the Upper Rienz/Rienza, the outlet was set at the location where the river enters the Val Pusteria valley floor. Due to the bilingual condition of South Tyrol, the toponyms are reported in German and Italian (see Table 1).

3. Materials & methods

This work builds upon a recently published data-driven approach (i.e. Steger et al., 2022) modified to fit the present regional scale context. To derive the final joint debris flow susceptibility–connectivity map, the approach can be divided into three main steps (Figure 2): (i) modeling debris flow release susceptibility, (ii) computation of a sediment connectivity index and (iii) derivation of a joined debris flow release susceptibility–connectivity map.

The approach herein applied was originally developed for the Stolla Creek catchment (basin area 40

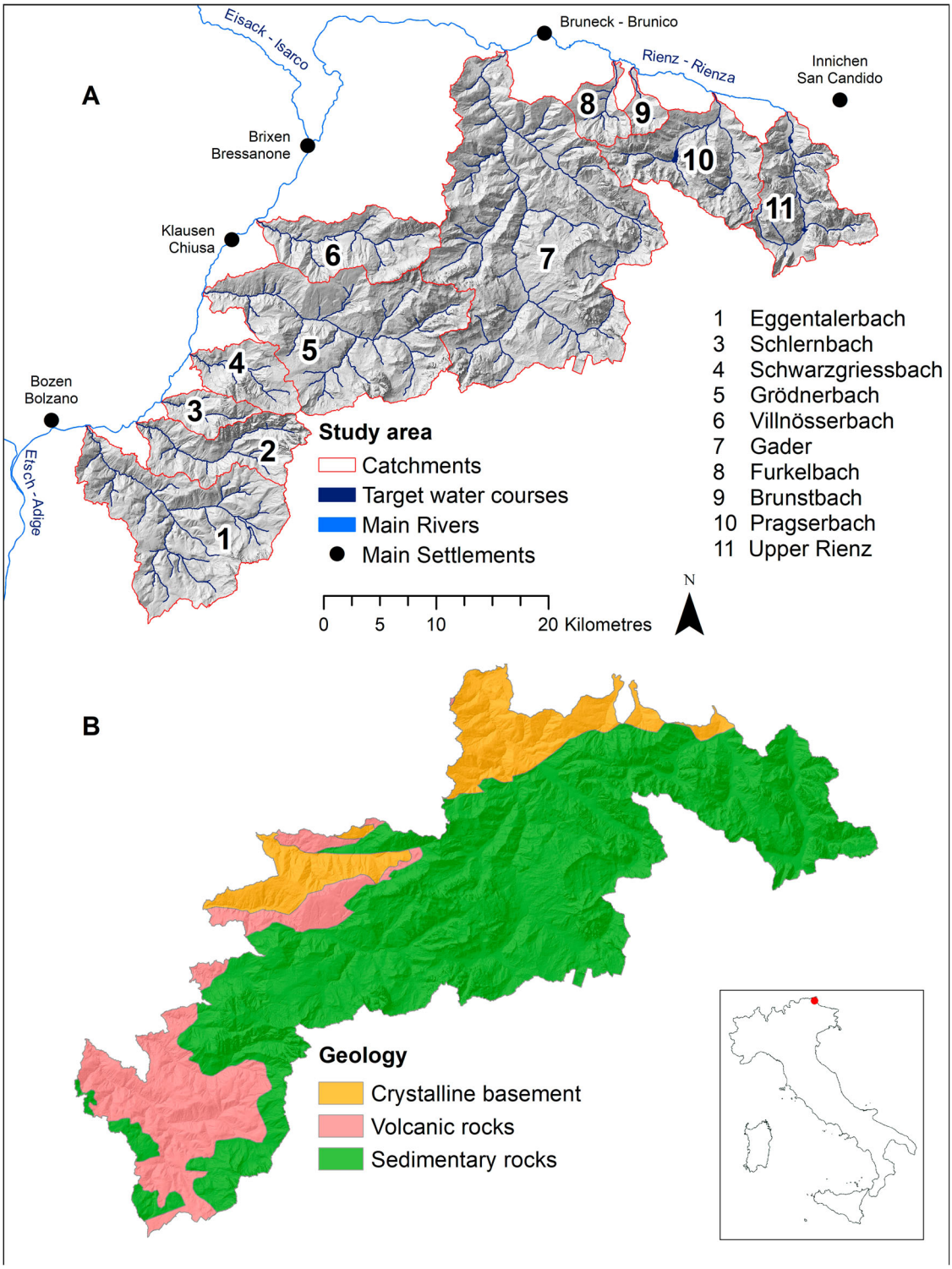

Figure 1. The study area of the present study is the part of the Dolomites located within South Tyrol (Autonomous Province of Bolzano-Bozen, northern Italy). The study area includes 11 river catchments draining to the Isarco/Eisack River, a major tributary of the Etsch/Adige River (A). The geology of these catchments can be summarized in three distinct categories: Crystalline basement in the north, porphyry in the south-west and sedimentary rocks in the man body of the Dolomites (B).

km^2), a lateral catchment of the Braies River (Figure 2 (A)). In August 2017, this area was affected by an extreme storm able to trigger more than 600 debris flows, part of which connected to the main channel (Scorpio et al., 2022; Steger et al., 2022). Numerous transferability tests of the original method (cf. Steger et al., 2022) revealed that the approach is suitable to be directly transferred within similar environments. Because the Stolla basin represents a paradigmatic catchment of the Dolomites (i.e. near-vertical rock walls composed of dolomite or limestone, extensive presence of talus slopes and cones at their base, forests and pastures underlain by weak sedimentary rocks) and is included in our study area, the already available pre-fitted models are deemed appropriate for the current upscaling to the whole Dolomitical region of South

Table 1. Main physiographic and morphologic characteristics of the study catchments.

Catchment German /Italian names	Catchment area (km^2)	Min elevation (m a.s.l.)	Max elevation (m a.s.l.)	Relief (m)	Average Slope (%)	Relative Unvegetated areas (%)	Relative Forest cover (%)	Relative Shrubland cover (%)	Relative Grassland cover (%)	Other* (%)
Eggentalerbach/Rio Ega	165.0	277	2837	2560	23.3	5.8	74.5	1.2	16.6	1.9
Tierserbach/ Rio Tires	64.5	310	2991	2681	31.6	14.0	60.9	2.5	20.6	2.0
Schlernbach/ Rio Sciliar	22.2	337	2559	2222	28.0	3.9	56.6	4.3	31.7	3.5
Schwarzgriessbach/Rio Nero	41.4	392	2653	2261	25.1	10.5	42.9	2.5	40.3	3.8
Grödnerbach/Rio Gadena	197.8	463	3173	2710	24.9	15.7	44.0	2.5	35.4	2.5
Villnösserbach/Rio Funes	72.8	532	3020	2489	28.3	10.4	64.8	1.3	21.6	2.0
Gader/Gadera	388.5	804	3119	2315	26.6	23.8	44.1	4.4	25.8	2.0
Furkelbach/Rio Furcia	23.4	973	2565	1592	25.2	9.8	57.3	2.1	25.6	5.2
Brunstbach/Rio Bruns	11.3	996	2563	1567	26.4	6.9	75.8	3.7	8.2	5.4
Pragserbach/Rio Braies	92.7	1112	3143	2030	30.0	31.4	34.6	10.2	22.7	1.1
Upper Rienz /Rienza	84.9	1199	2991	1791	33.4	36.4	34.7	14.2	13.2	1.4
Total area	1164.3	277	3173	2896	27.0	18.7	49.9	4.4	24.8	2.1

*See Table 2.

Tyrol. The debris flows that occurred in the Stolla catchment during the extreme event of 2017 were mapped in the work of Scorpio et al. (2022). As in the original approach by Steger et al. (2022) (hereafter named Stolla model), also the present work employs these previously mapped debris flows to train the statistical model for analyzing the connectivity within the present study area and the model for assessing debris flow initiation susceptibility. In contrast to the original study, the present work embraces a different approach to determining the water bodies as a target for the connectivity analysis (see section 3.3). Thus, a re-labeling in terms of (dis-)connectivity of the previously mapped debris flows and a re-calibration of the underlying logistic regression model had to be performed.

3.1. DTM and orthophotos

A LiDAR-derived Digital Terrain Model (DTM) with a 5 m resolution was used to create a variety of topographic indices. The 5 m DTM was derived by averaging the values within a moving window from a 2.5 m resolution DTM (acquired in 2005/2006) provided by the Autonomous Province of Bolzano-Bozen. A 5 m resolution DTM was considered a good compromise to preserve an accurate morphological representation over a large area without excessively overloading the data processing. Moreover, the 5 m resolution reduces the potential for an overestimation of disconnections resulting from small-scale topography (Lisenby & Fryirs, 2017) and allows to be consistent with the original development of the approach (Steger et al., 2022).

Orthophotos of the study area were taken in 2014 with a resolution of 0.2 m.

3.2. Assessment of debris flow release susceptibility

The susceptibility to debris flow release areas was determined by data-driven modeling within the software 'R' (R Core Team, 2017). The general procedure described in Steger et al. (2022) was followed and spatially transferred to the predisposing factor maps (Figure 2), with the difference that the final binary susceptibility map was further smoothened by applying a 3 × 3 cells modal filter. In this way, isolated single cells and noisy appearing spatial patterns were minimized. To create the underlying spatial predictions (i.e. the continuous debris flow release probability scores), the predict function of the previously fitted Stolla model was applied to the seven regional predisposing factor maps. Six of these maps, namely slope angle (Figure 3(A)), normalized height index (the relative slope position in the study area) (Figure 3(B)), planform curvature (Figure 3(C)), profile curvature (Figure 3(D)), a topographic roughness index (slope roughness) (Figure 3(E)) and a topographic wetness index (Figure 3(F)), describe the topography of the area. These factors were derived from the 5 m DTM within the SAGA GIS software (ver. 8.1.1; Conrad et al., 2015). In addition, a land cover was extracted from the Land-use Information System South Tyrol (LISS, 2013) (see Table 1) and rasterized to the required 5 m resolution. The land use classes were grouped into five classes, i.e. bare soil, grassland, shrubland, forest, and others (Table 2, Figure 3(G)). The class 'other' was not present within the original training area in the Stolla catchment and therefore also not considered for the regional scale spatial predictions.

To determine the predictive power of the model the Area Under the Receiving Operating Characteristic (AUROC) curve was used (Lima et al., 2022; Steger et al., 2020). The AUROC represents a standard metric for evaluating the results of probability-based binary classifications. An AUROC of 0.5 represents a random classification, while an AUROC of 1 indicates perfect separation. According to Hosmer et al. (2013), an AUROC above 0.7 indicates acceptable discrimination, and above 0.8 suggests excellent separation.

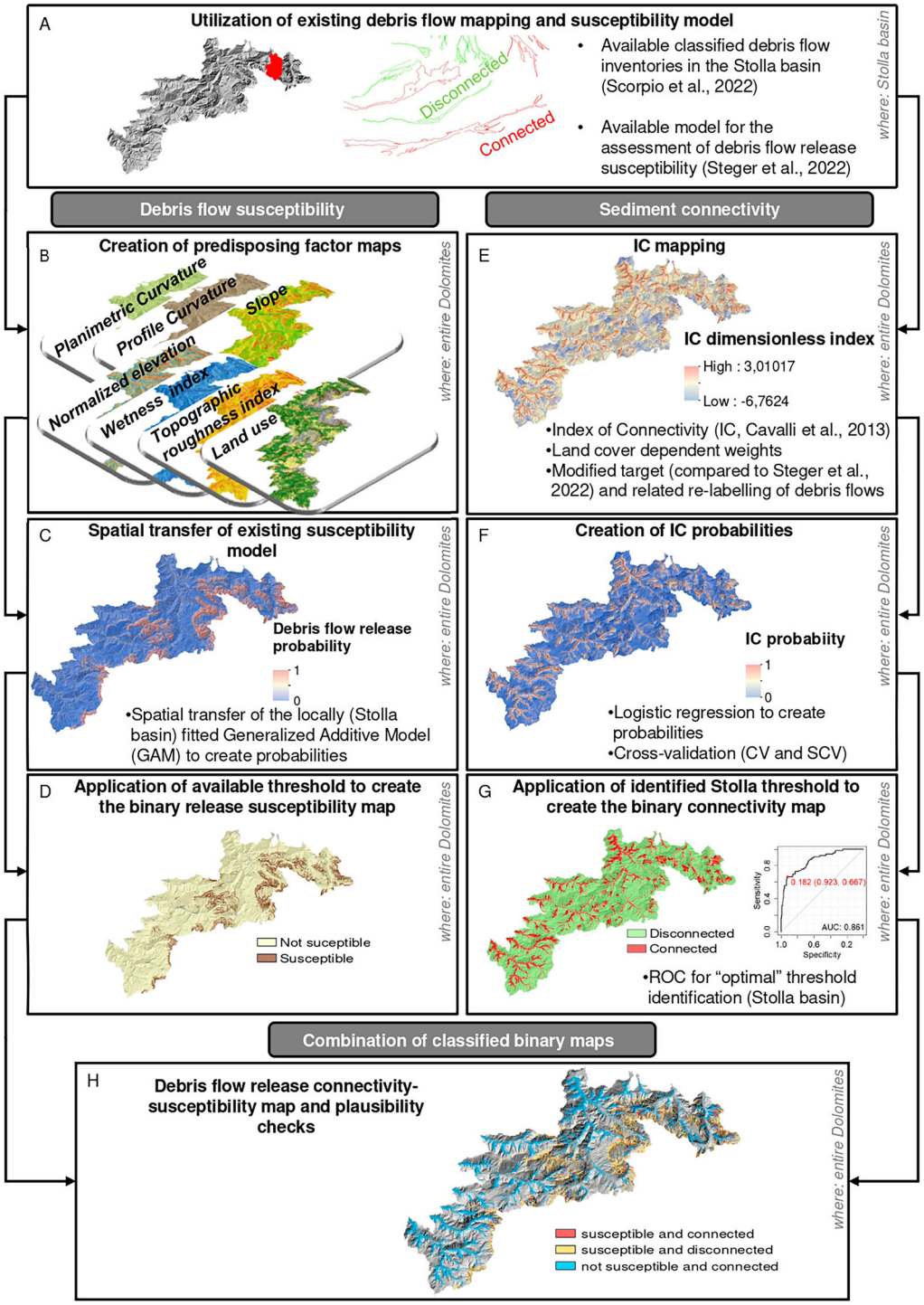

Figure 2. Flowchart of the methodological framework. Existing debris flow mapping and the existing model in the Stolla basin (Steger et al., 2022) were used to derive the susceptibility to debris flow initiation and sediment connectivity (A). For assessing the debris flow susceptibility 7 predisposing factors (slope angle, plan curvature, profile curvature, topographic wetness index, slope roughness, normalized height index and land use; B) were used to model debris flow release probability (C) on which an identified threshold was applied to create a binary map (susceptible and not susceptible; D). The connectivity to the established target was assessed by identifying the index of connectivity (IC) within the whole study area (E). The IC probabilities were created (F) and the threshold for creating a binary map (connected, disconnected) was identified and applied (G). The binary maps were spatially overlaid to create the final susceptibility-connectivity map (H).

3.3. Assessment of debris flow connectivity

To assess sediment connectivity a geomorphometric index was applied (index of connectivity IC, Cavalli et al., 2013). This index describes the relative potential of sediment from any area of the catchment to reach a selected target (e.g. a watercourse or a river outlet). The IC is estimated starting from a DTM by computing morphometric parameters. A weight factor, that could be based on surface roughness (Cavalli et al., 2008) or land use properties (e.g. Borselli et al., 2008; Persichillo et al., 2018), is applied to represent the impedance to sediment fluxes.

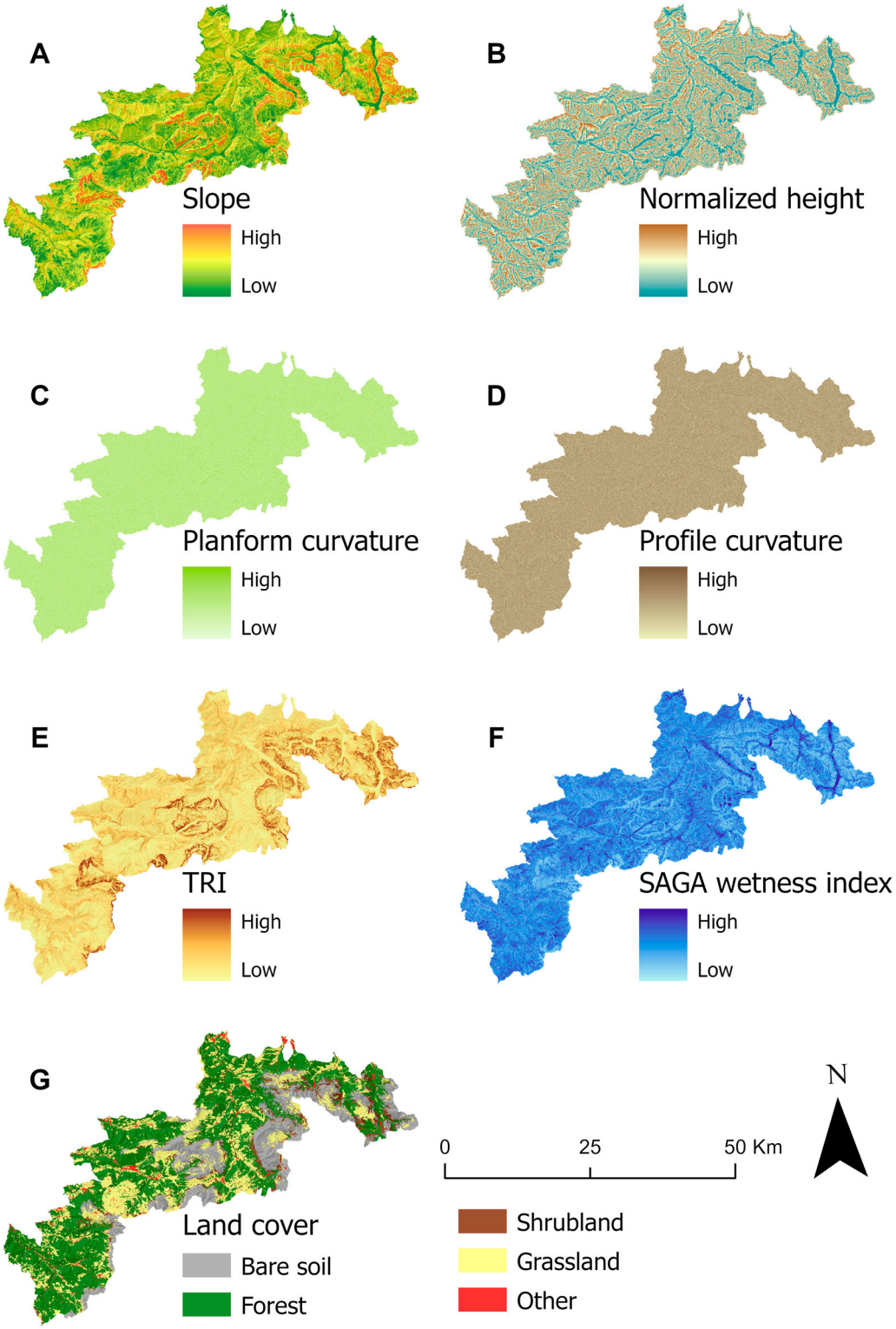

Figure 3. The seven predisposing factors for the debris flow susceptibility analysis across the Dolomites in South Tyrol: Slope angle (A), Normalized height (B) and Planform curvature (C), Profile curvature (D), Topographic Roughness Index (E), SAGA Wetness index (F), and Land cover (G).

In the present work, the main water bodies (main channels and lakes, Figure 1(A)) within the study area were set as 'targets' for the connectivity analysis, i.e. the final ending point(s) to which sediment transfer is considered to occur. The river network was delineated based on flow accumulation derived from the DTM. The threshold for the drainage area was established at 1.5 km² to match the length of Stolla Creek as reported in the earlier studies by Scorpio et al. (2022) and Steger et al. (2022). In contrast to the original works where the river network was trimmed to include only the main channels of the catchments, in the present analyses also tributaries that drain major lateral valleys were set as targets. Polylines that resulted in being too short to fully represent the tributary channels were manually deleted and thus

Table 2. Land cover is divided into five classes and categories, respectively.

Original land use map (LISS, 2013)	Reclassified land cover classes	Land cover category	Manning's *n* value	Weight factor
Bare rock	Bare soil	1	0.050	0.950
Unvegetated scree	Bare soil	1	0.150	0.850
Forest	Forest	2	0.400	0.600
Shrubland with mugo pine (*Pinus mugo)*	Shrubland	3	0.300	0.700
Shrubland	Shrubland	3	0.300	0.700
Grassland	Grassland	4	0.100	0.900
Grasslands with trees	Grassland	4	0.200	0.800
Artificial surfaces	Other	5	0.020	0.980
Cultivated area	Other	5	0.200	0.800
Vineyard	Other	5	0.200	0.800
Orchard	Other	5	0.200	0.800
Other agricultural use	Other	5	0.200	0.800
Wetlands	Other	5	0.001	0.999
Water bodies	Other	5	0.001	0.999

Note: Each land cover was attributed with Overland flow Manning's n Roughness Values and the according Weight factor.

excluded from being a target to focus the analysis only on channels draining main valleys. The final target water bodies – in the form of polygons – were obtained by applying a 10 m buffer (average channel width in the study area) to the polylines of the selected rivers. Lakes were manually included in the target polygon.

The IC within the study area was computed using the stand-alone software SedInConnect (Crema & Cavalli, 2018). The topographic data used as input in IC computation was the 5 m DTM (see section 3.1). Before the application, pits in the DTM were removed using the TauDEM toolbox in the ArcMap software (ESRI ArcGIS ver.10.8)

Steger et al. (2022), used the standard weight factor implemented in the SedInConnect software, i.e. DTM-derived surface roughness. However, at the regional scale a much larger variability of land use is present, and, as suggested by different authors (e.g. Goldin, 2015; Martini et al., 2019; Persichillo et al., 2018), in this work, the overland flow Manning's *n* was instead utilized to estimate the weight factor. It is possible to estimate Manning's *n* value through empirical tables, considering the land cover of a given area. In this study, Manning's *n* values were applied using the values proposed by Goldin (2015) as a reference to calculate the final weight factor (W, Table 2) as follows:

$$W = 1 - n$$

The resulting IC map was transformed into a binary map, representing areas structurally connected to the target water courses and areas which are disconnected. The threshold for discriminating the IC between the two groups (connected vs. disconnected) was derived by training a one-predictor binomial Generalized Linear Model (GLM), namely, logistic regression (Hosmer et al., 2013), based on the labeled debris flow release locations (binary response) and the IC index (predictor variable). In particular, the debris flows mapped in the Stolla catchment by Scorpio et al. (2022) were used for labeling debris flow release points according to their connectivity status (i.e. connected or disconnected) with regard to the updated target water courses. The labeling was based on empirical comparisons of orthophotos and DTMs acquired before and after the rainstorm events of 2017. The exact workflow and results are described in Scorpio et al. (2022). As performed by Steger et al. (2022), the coupling or decoupling of the debris flow initiation areas with respect to the receiving main channel was evaluated based on a visual inspection of orthophotos regarding debris flow deposits: if debris flow sediments clearly reached the main channel, the related debris flow polygon was classified as connected and vice versa.

The predict function of the newly trained logistic regression model was then used to derive the subsequent continuously scaled map (i.e. IC probabilities; Figure 2 (F)) as a function of the spatial distribution of the IC map (Figure 2(E)). This map was then categorized into the two groups of interest, i.e. connected vs. disconnected (Figure 2(G)). The classification related to the probability-based debris flow connectivity model was evaluated using the AUROC metric (cf. Section 3.2).

3.4. Maps combination

The resulting binary debris flow release susceptibility map (susceptible vs. not susceptible) and the binary connectivity map (connected vs. disconnected) were spatially intersected to obtain the final joint susceptibility–connectivity map (Figure 2(H), Main Map). To accomplish this, the maps were spatially overlaid and four classes – susceptible and connected, susceptible but not connected, not susceptible but connected and not susceptible and not connected – were visualized. To enhance visual interpretability, the fourth class (not susceptible and not connected) and the landcover class 'other' were set to transparent in the final maps. The plausibility of the susceptibility–connectivity map was qualitatively checked for the whole area by overlaying the mapped categories to

the orthophotos and visually examined for concurrence and geomorphological plausibility. Furthermore, the final map was compared to the mapped predictors in order to gain a better overview of the potential reasons for the final classification.

4. Results and discussion

4.1. Debris flow susceptibility

To evaluate the susceptibility to debris flow initiation the model developed by Steger et al. (2022) for the Stolla basin was expanded to a regional scale. It is based on six statistically significant parameters: slope angle, normalized height, planform curvature, profile curvature, land cover and the interaction between surface roughness and wetness index (Figure 3). According to this model, the relative probability for debris flow initiation was mapped to be highest within a Dolomitic catchment if the topographic setting is represented by medium inclined slopes (around 40°, Figure 4(A)), medium relative hillslope positions below the typical Dolomitic rock walls (normalized height peaks at around 0.5, Figure 4(B)) and concave shaped terrain (negative plan and profile curvature values, Figure 4(C,D)). Furthermore, bare surface areas were associated with the highest debris flow susceptibility, followed by grasslands and shrublands. Forested terrain, in contrast, was related to the lowest chance to represent a debris flow initiation location (Figure 4(E)). The interaction terms describe that in cases where rough terrain spatially overlaps with a high topographic wetness index, a higher debris flow release susceptibility can be expected (Figure 4(F)).

From a geomorphic viewpoint, these relationships appear to be plausible and not a direct result of model artifacts or biased debris flow mapping (Steger et al., 2016). For instance, the shown nonlinear relationship between debris flow release and slope angle (Figure 4(A)) can be considered plausible, since accumulated soils are known to lose structural stability with increasing slope angles due to gravitational forces. Beyond a slope angle of 40°, these forces might become too strong for debris to stabilize and accumulate. The normalized height variable shows similar nonlinear behavior. Debris flow initiation is modeled to be highest at medium relative heights, as in the Dolomites lower positions are typically characterized by denser vegetation while at highest positions steep rock faces without debris accumulation are prevalent. Debris and water tend to accumulate in concave-shaped morphologies, thus both variables

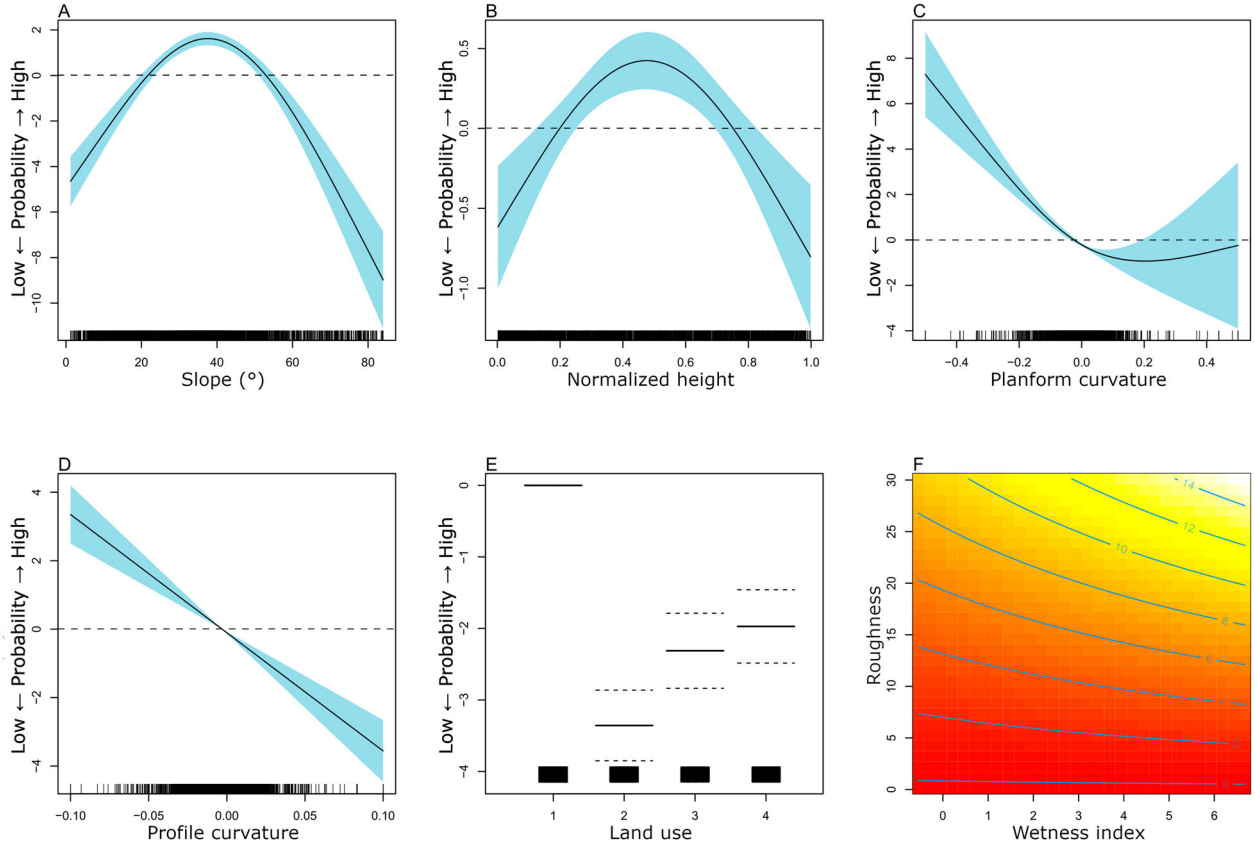

Figure 4. Relationships that depict the estimated associations between debris flow release and environmental features derived via the application of the Stolla model by Steger et al. (2022). Note that for the plots A-D, y-axis values above 0 point to an above-average probability of debris flow initiation and vice versa. Plot E points to the estimated chance of debris flow initiation with respect to the chosen reference land cover class. The colors in plot F depict increasing probabilities (from red to white) as a function of the interaction between Roughness (y-axis) and Wetness index (x-axis).

for planform and profile curvature reasonably predicted the highest probability of the triggering of sediment movement for such landforms.

The application of these modeled relationships allowed us to assess and map the probability of debris flow release for the whole study area (Figure 2(A)). The resulting map basically reflects the previously discussed modeled relationships and shows that the areas with the highest probabilities lie on the upper hillslopes of the mountain ridges, but it also clearly shows, that the steep mountainous rock walls are not susceptible to debris flow initiation.

Using the predictors to discriminate between areas susceptible and not susceptible to debris flow initiation, this model shows a high performance (AUROC 0.92; Figure 5(A)). For creating the binary map (see Main Map, Map of Susceptibility) of these two classes, a probability cutpoint of 0.34 was identified. Considering the abovementioned variables, around 10% of the spatial extent of the Dolomites of South Tyrol turns out susceptible to debris flow initiation.

The mapping of the modeled susceptibility of debris flow initiation identifies areas with elevated potential for such phenomena. In the South Tyrolean Dolomites it is evident, that the western parts are less susceptible than the central and eastern sectors. This can be explained by the prevalent geological (Figure 1(B)) and topographic setting. Catchments in the east are largely characterized by sedimentary rocks, that are prone to weather and thus provide loose soils susceptible to debris flow initiation. Furthermore, steeper slopes (Figure 3(A)), a higher topographic roughness index (Figure 3(E)), and a lower percentage of forest cover (Table 1, Figure 3(G)) characterize the eastern catchments. However, there are catchments and areas within catchments that differ from this generalized assumption, highlighting the need for further analysis of single catchments for precise results.

4.2. Debris flow connectivity

In this work, information on 585 debris flows (represented by 611 point locations) was used to train the statistical model. Due to the modification of the target river network, a re-labeling of the connectivity of the debris flows had to be performed and 50 (8.5%) were categorized as connected. The original work by Steger et al. (2022), where only the main water course was used as a target, labeled only 39 (6%) debris flows as connected.

IC values for connected debris flows were considerably higher than for disconnected (median −1.85 and −2.93, respectively; Figure 6(A)). For separating connected and disconnected debris flows and thus creating a binary map (see Main Map, Map of Connectivity), the optimal cutpoint was determined to be −2.19, whereas all areas with higher values were labeled as connected (Figure 6(B)). The logistic regression model to discriminate between connected and disconnected areas performed well (AUROC 0.86; Figure 5(B)), which was confirmed by tests based on spatial (SCV, median AUROC 0.87) and non-spatial (CV, median AUROC 0.87) cross-validation.

The IC cutpoint determined for the Dolomites of the South Tyrol differs from the value observed in the Stolla basin only, which was −3.21 (Steger et al., 2022). This results in fewer areas within the catchment being considered structurally connected to the river network. The discrepancy between the two identified values can be attributed the different target chosen in this study and the subsequent changes in the (dis-)connectivity classification of the mapped debris flows. With the identified cutpoint of −2.19,

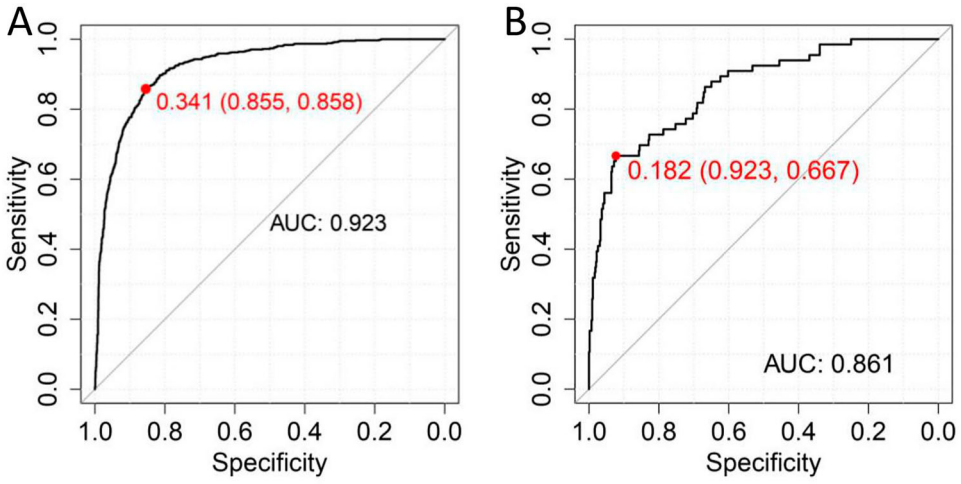

Figure 5. ROC-curve, fitting performance (AUC) and associated 'optimal' threshold (red point) for separating susceptible from non-susceptible areas (A) and connected from disconnected areas (B).

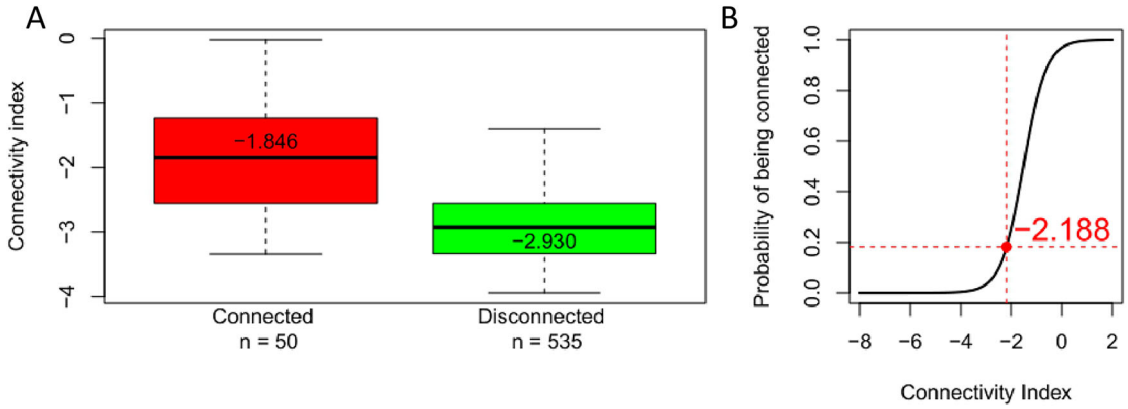

Figure 6. IC values for debris flows labeled as connected and disconnected (A). The significant difference between median values allows for good discrimination between the two categories. This allowed identifying the optimal IC value for the cutpoint to separate connected and disconnected areas (B).

around 18% of the modeled area is predicted to be connected.

4.3. The joint susceptibility-connectivity map

The joined map of the binary IC and susceptibility maps shows areas that are susceptible and connected, susceptible but disconnected, and not susceptible and disconnected in terms of debris flow release (see Main Map). Areas that are both susceptible and connected to the main watercourse cover only 1.7% of the areal extent of the study area, 8.2% is susceptible but disconnected, and 16.5% is potentially connected but not susceptible to debris flow initiation.

Overlaying and comparing the joint susceptibility–connectivity map and the orthophoto indicates that the visually interpretable geomorphic setting is represented well by the categorization (Figure 7). Figure 7(A) depicts the channelized pattern of areas predicted to be susceptible and connected well. The eroded debris flow channels are clearly visible and reach the target water course. Areas between the channels, even though they have a similar topographic setting but are covered by shrubs and trees, mainly show no visible debris flow initiation and transportation and are thus justifiably categorized as not susceptible and connected. Comparing these patterns to Figure 7(B), it can be observed, that the areas susceptible to debris flow initiation are in the steeper areas of the hillslopes. The flatter areas closer to the watercourse are not prone to debris flow initiation and depositions are visible on the orthophoto. However, these depositions do reach the watercourse, and thus it is clear that these areas are correctly categorized as connected. Areas in which clear debris flow initiation and deposition are visible are shown in Figure 7(C). The channelized erosions of debris flows can be easily identified on the orthophoto, as well as the depositions of these mass movements. The sediments do not reach the watercourse and thus these areas are classified as susceptible and disconnected. In Figure 7(D) an area with large clear cuts for pastures and ski slopes is shown. The fact that there are no obstacles between them and the watercourse, as well their proximity to the channel, render them ‘connected’. Their limited slope and the stabilisation imparted by the grass cover prevent debris flows from being triggered and thus these areas are deemed to be not susceptible.

This study shows, that even if substantial parts of an analyzed area are susceptible to debris flow initiation, not all triggered sediments are necessarily transferred to the fluvial system. In fact, only a small part of areas considered susceptible are structurally connected to the river network. The potential decoupling of the hillslopes has already been highlighted in several studies (e.g. Schopper et al., 2019; Scorpio et al., 2018; Surian et al., 2016). This reinforces our approach and gives emphasis to the importance of combining both susceptibility and connectivity analyses for assessing sediment cascades from the hillslopes to the fluvial system.

5. Conclusion

This study built upon the work of Steger et al. (2022), in which a novel methodological approach to categorize areas within mountain catchments according to their susceptibility to debris flow initiation and structural connectivity to the main river network was developed and tested. In the present work, this approach has been adapted to a regional-scale context and tested. The adapted model shows high performance in discriminating between susceptible and non-susceptible areas (AUROC 0.92), as well as between areas connected and disconnected to the main water courses (AUROC 0.86). Visual comparisons of predicted debris flow susceptibility and (dis-)connectivity with observed real events indicate a spatial agreement and plausible results.

The ease of implementation of the proposed approach, in addition to its limited requirement in

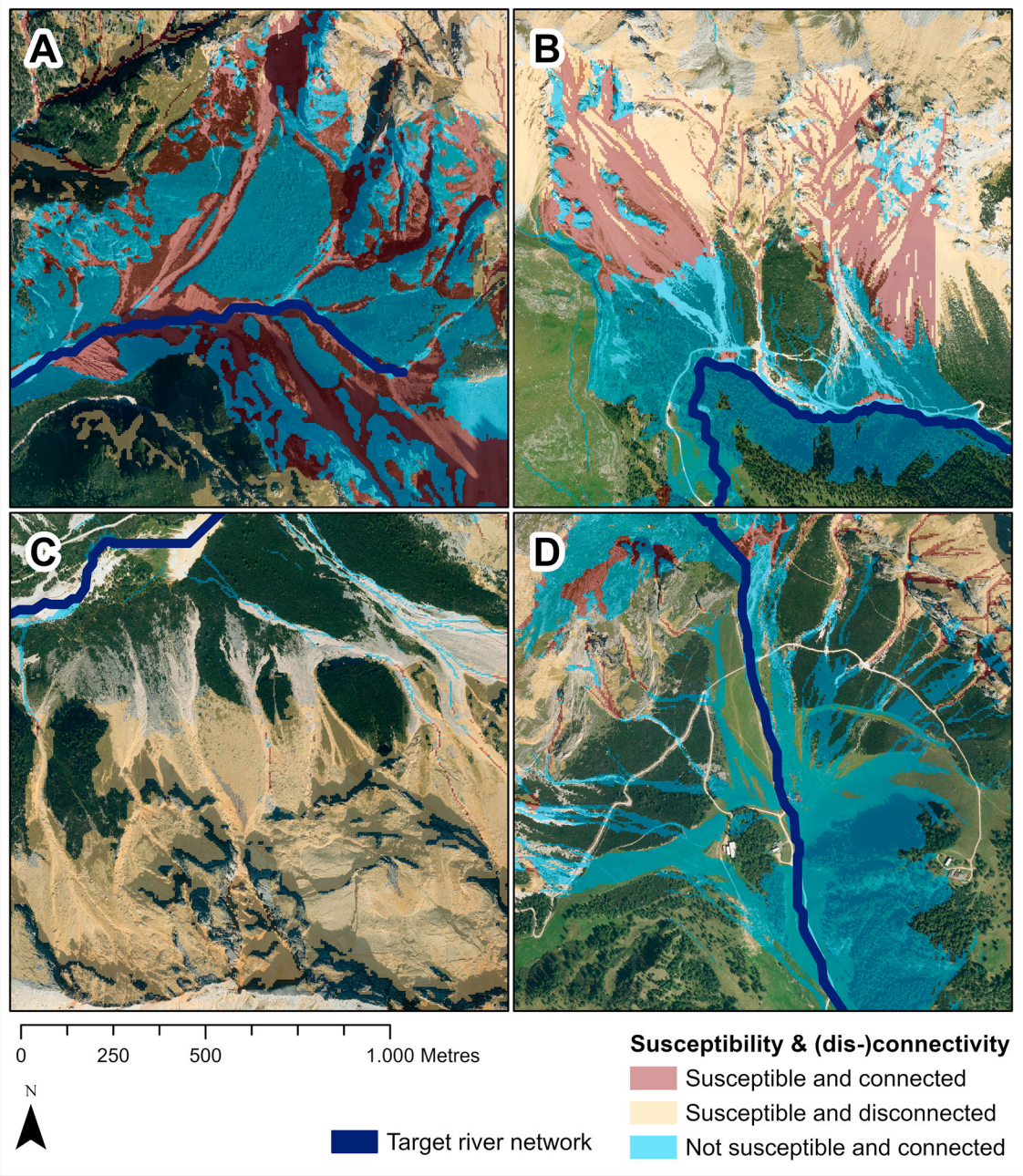

Figure 7. Selected examples for visual inspection of the joined susceptibility-connectivity map, overlaid onto the orthophoto of the study area.

terms of input data sets, makes it a valuable tool to carry out preliminary hazard mapping at the regional scale, as well as to inform about best strategies to quantitatively assess and then manage sediment transport in alpine catchments. Indeed, the relatively straightforward application of the model can help to provide a basic understanding of where within a region, or specific catchments, efforts to manage sediments need to be focused. The general overview provided by the mapping process presented in this work can reduce the time needed to identify 'hot spots' where sediment management is most needed, in which consequently more intensive analyses and assessments should be performed. Even though this study shows that the implementation of this new approach on a regional scale delivers plausible results, further analyses in single, selected catchments can be recommended.

Software

The elaborations of the topographic data and the land use map, as well as the identification of the selected watersheds and the selected target, were performed in ArcMap within the ESRI ArcGIS 10.8 environment. Predictors for the susceptibility analysis were derived from the DTM using the SAGA GIS software. The connectivity analysis was performed via the stand-alone software SedInConnect. Data for this analysis was prepared in ArcMap using the TauDEM toolbox. The modeling of the susceptibility and the identification of

thresholds for the creation of binary maps for susceptibility and connectivity, as well as the combination of these two maps, were performed in R Studio. The final layout of the Main Map was prepared in ArcMap.

Geolocation information

The coordinates of the lower left corner (south-west) of the study area are 46.313650, 11.370327; the ones from the upper right corner (north-east) are 46.795159, 12.325499.`

Summary for social media

The study presents the application of a novel approach to assess susceptibility to debris flow release areas and their potential structural connectivity at the regional scale. The analysis can assist sediment transport analyses and hazard zone mapping at a higher detail.

Acknowledgements

This research was founded by the project 'CoupEvent: Hillslope – Channel coupling during extreme events in South Tyrol', supported by the Autonomous Province of Bozen-Bolzano (Bandi per la mobilitá di ricercatrici e ricercatori 2019; L.P. 14. Mobility, Province BZ funding /Project). The authors thank the editor and reviewers for their valuable comments that helped improving the manuscript and the map.

Disclosure statement

No potential conflict of interest was reported by the author(s).

Funding

The present work has been performed in the framework of the project 'CoupEvent: Hillslope – Channel coupling during extreme events in South Tyrol', funded by the Autonomous Province of Bozen-Bolzano (Bandi per la mobilitá di ricercatrici e ricercatori 2019; L.P. 14. Mobility, Province BZ funding /Project); and it was supported by the found FAR2022 – University of Modena and Reggio Emilia. 2014 orthophotos and the 2005/2006 DTM were made available by the Department of Geographic Informatics and Statistics of the Autonomous Province of Bolzano-Bozen.

Data availability statement

Data is available on request from the authors.

References

Borselli, L., Cassi, P., & Torri, D. (2008). Prolegomena to sediment and flow connectivity in the landscape: A GIS and field numerical assessment. *CATENA*, *75*(3), 268–277. https://doi.org/10.1016/j.catena.2008.07.006

Bracken, L. J., Turnbull, L., Wainwright, J., & Bogaart, P. (2015). Sediment connectivity: A framework for understanding sediment transfer at multiple scales. *Earth Surface Processes and Landforms*, *40*(2), 177–188. https://doi.org/10.1002/esp.3635

Bracken, L. J., Wainwright, J., Ali, G. A., Tetzlaff, D., Smith, M. W., Reaney, S. M., & Roy, A. G. (2013). Concepts of hydrological connectivity: Research approaches, pathways and future agendas. *Earth-Science Reviews*, *119*, 17–34. https://doi.org/10.1016/j.earscirev.2013.02.001

Brardinoni, F., & Hassan, M. A. (2006). Glacial erosion, evolution of river long profiles, and the organization of process domains in mountain drainage basins of coastal British Columbia. *Journal of Geophysical Research: Earth Surface*, *111*(F01013). https://doi.org/10.1029/2005JF000358

Brardinoni, F., Mao, L., Recking, A., Rickenmann, D., & Turowski, J. M. (2015). Morphodynamics of steep mountain channels. *Earth Surface Processes and Landforms*, *40*(11), 1560–1562. https://doi.org/10.1002/esp.3742

Brierley, G., Fryirs, K., & Jain, V. (2006). Landscape connectivity: The geographic basis of geomorphic applications. *Area*, *38*(2), 165–174. https://doi.org/10.1111/j.1475-4762.2006.00671.x

Cavalli, M., Goldin, B., Comiti, F., Brardinoni, F., & Marchi, L. (2017). Assessment of erosion and deposition in steep mountain basins by differencing sequential digital terrain models. *Geomorphology*, *291*, 4–16. https://doi.org/10.1016/j.geomorph.2016.04.009

Cavalli, M., Tarolli, P., Marchi, L., & Dalla Fontana, G. (2008). The effectiveness of airborne LiDAR data in the recognition of channel-bed morphology. *CATENA*, *73*(3), 249–260. https://doi.org/10.1016/j.catena.2007.11.001

Cavalli, M., Trevisani, S., Comiti, F., & Marchi, L. (2013). Geomorphometric assessment of spatial sediment connectivity in small Alpine catchments. *Geomorphology*, *188*, 31–41. https://doi.org/10.1016/j.geomorph.2012.05.007

Cavalli, M., Vericat, D., & Pereira, P. (2019). Mapping water and sediment connectivity. *Science of the Total Environment*, *673*, 763–767. https://doi.org/10.1016/j.scitotenv.2019.04.071

Cislaghi, A., & Bischetti, G. B. (2019). Source areas, connectivity, and delivery rate of sediments in mountainous-forested hillslopes: A probabilistic approach. *Science of the Total Environment*, *652*, 1168–1186. https://doi.org/10.1016/j.scitotenv.2018.10.318

Conrad, O., Bechtel, B., Bock, M., Dietrich, H., Fischer, E., Gerlitz, L., Wehberg, J., Wichmann, V., & Böhner, J. (2015). System for Automated Geoscientific Analyses (SAGA) v. 2.1.4. *Geoscientific Model Development*, *8*(7), 1991–2007. https://doi.org/10.5194/gmd-8-1991-2015

Crema, S., & Cavalli, M. (2018). SedInConnect: a stand-alone, free and open source tool for the assessment of sediment connectivity. *Computers & Geosciences*, *111*, 39–45. https://doi.org/10.1016/j.cageo.2017.10.009

Crespi, A., Matiu, M., Bertoldi, G., Petitta, M., & Zebisch, M. (2021). A high-resolution gridded dataset of daily temperature and precipitation records (1980-2018) for Trentino-South Tyrol (north-eastern Italian Alps). *Earth System Science Data*, *13*(6), 2801–2818. https://doi.org/10.5194/essd-13-2801-2021

Fryirs, K. A., Brierley, G. J., Preston, N. J., & Kasai, M. (2007). Buffers, barriers and blankets: The (dis)connectivity of catchment-scale sediment cascades. *CATENA*, *70*(1), 49–67. https://doi.org/10.1016/j.catena.2006.07.007

Goetz, J., Kohrs, R., Parra Hormazábal, E., Bustos Morales, M., Araneda Riquelme, M. B., Henríquez, C., & Brenning, A. (2021). Optimizing and validating the Gravitational

Process Path model for regional debris-flow runout modelling. *Natural Hazards and Earth System Sciences*, *21*(8), 2543–2562. https://doi.org/10.5194/nhess-21-2543-2021

Goldin, B. (2015). *Geomorphometric analysis and sediment dynamics in mountainous basins: Spatial and temporal scales. (Doctoral thesis). università*. degli Studi di Padova.

Heckmann, T., Cavalli, M., Cerdan, O., Cerdan, O., Foerster, S., Javaux, M., Lode, E., Smetanová, A., Vericat, D., & Brardinoni, F. (2018). Indices of sediment connectivity: Opportunities, challenges and limitations. *Earth-Science Reviews*, *187*, 77–108. https://doi.org/10.1016/j.earscirev.2018.08.004

Heckmann, T., Gegg, K., Gegg, A., & Becht, M. (2014). Sample size matters: Investigating the effect of sample size on a logistic regression susceptibility model for debris flows. *Natural Hazards and Earth System Sciences*, *14*(2), 259–278. https://doi.org/10.5194/nhess-14-259-2014

Hooke, J. (2003). Coarse sediment connectivity in river channel systems: A conceptual framework and methodology. *Geomorphology*, *56*(1-2), 79–94. https://doi.org/10.1016/S0169-555X(03)00047-3

Hosmer, D. W., Lemeshow, S., & Sturdivant, R. X. (2013). *Applied logistic regression* (3rd ed.). Wiley.

Lima, P., Steger, S., Glade, T., & Murillo-García, F. G. (2022). Literature review and bibliometric analysis on data-driven assessment of landslide susceptibility. *Journal of Mountain Science*, *19*(6), 1670–1698. https://doi.org/10.1007/s11629-021-7254-9

Lisenby, P. E., & Fryirs, K. A. (2017). 'Out with the Old?' Why coarse spatial datasets are still useful for catchment-scale investigations of sediment (dis)connectivity. *Earth Surface Processes and Landforms*, *42*(10), 1588–1596. https://doi.org/10.1002/esp.4131

LISS. (2013). Land-use information in South Tyrol: Update, harmonization with European Standards and integration of research results (© Autonome Provinz Bozen – Südtirol | 28.0.1 Landeskartographie und Koordination der Geodaten).

Martini, L., Picco, L., Iroumé, A., & Cavalli, M. (2019). Sediment connectivity changes in an Andean catchment affected by volcanic eruption. *Science of the Total Environment*, *692*, 1209–1222. https://doi.org/10.1016/j.scitotenv.2019.07.303

Persichillo, M. G., Bordoni, M., Cavalli, M., Crema, S., & Meisina, C. (2018). The role of human activities on sediment connectivity of shallow landslides. *CATENA*, *160*, 261–274. https://doi.org/10.1016/j.catena.2017.09.025

R Core Team. (2017). R: A Language and Environment for Statistical Computing.

Reichenbach, P., Rossi, M., Malamud, B. D., Mihir, M., & Guzzetti, F. (2018). A review of statistically-based landslide susceptibility models. *Earth-Science Reviews*, *180*, 60–91. https://doi.org/10.1016/j.earscirev.2018.03.001

Schopper, N., Mergili, M., Frigerio, S., Cavalli, M., & Poeppl, R. (2019). Analysis of lateral sediment connectivity and its connection to debris flow intensity patterns at different return periods in the Fella River system in northeastern Italy. *Science of the Total Environment*, *658*, 1586–1600. https://doi.org/10.1016/j.scitotenv.2018.12.288

Schrott, L., Hufschmidt, G., Hankammer, M., Hoffmann, T., & Dikau, R. (2003). Spatial distribution of sediment storage types and quantification of valley fill deposits in an alpine basin, Reintal, Bavarian Alps, Germany. *Geomorphology*, *55*(1-4), 45–63. https://doi.org/10.1016/S0169-555X(03)00131-4

Schuerch, P., Densmore, A. L., McArdell, B. W., & Molnar, P. (2006). The influence of landsliding on sediment supply and channel change in a steep mountain catchment. *Geomorphology*, *78*(3-4), 222–235. https://doi.org/10.1016/j.geomorph.2006.01.025

Scorpio, V., Cavalli, M., Steger, S., Crema, S., Marra, F., Zaramella, M., Borga, M., Marchi, L., & Comiti, F. (2022). Storm characteristics dictate sediment dynamics and geomorphic changes in mountain channels: A case study in the Italian Alps. *Geomorphology*, *403*, 108173. https://doi.org/10.1016/j.geomorph.2022.108173

Scorpio, V., Crema, S., Marra, F., Righini, M., Ciccarese, G., Borga, M., Cavalli, M., Corsini, A., Marchi, L., Surian, N., & Comiti, F. (2018). Basin-scale analysis of the geomorphic effectiveness of flash floods: A study in the northern Apennines (Italy). *Science of the Total Environment*, *640–641*, 337–351. https://doi.org/10.1016/j.scitotenv.2018.05.252

Spiekermann, R. I., Smith, H. G., McColl, S., Burkitt, L., & Fuller, I. C. (2022). Development of a morphometric connectivity model to mitigate sediment derived from storm-driven shallow landslides. *Ecological Engineering*, *180*, 106676. https://doi.org/10.1016/j.ecoleng.2022.106676

Steger, S., Brenning, A., Bell, R., Petschko, H., & Glade, T. (2016). Exploring discrepancies between quantitative validation results and the geomorphic plausibility of statistical landslide susceptibility maps. *Geomorphology*, *262*, 8–23. https://doi.org/10.1016/j.geomorph.2016.03.015

Steger, S., & Kofler, C. (2019). Statistical modeling of landslides. In Hamid Reza Pourghasemi & Candan Gokceoglu (Eds.), *Spatial Modeling in GIS and R for Earth and Environmental Sciences* (pp. 519–546). Elsevier. https://doi.org/10.1016/b978-0-12-815226-3.00024-7

Steger, S., Schmaltz, E., & Glade, T. (2020). The (f)utility to account for pre-failure topography in data-driven landslide susceptibility modelling. *Geomorphology*, *354*, 107041. https://doi.org/10.1016/j.geomorph.2020.107041

Steger, S., Scorpio, V., Comiti, F., & Cavalli, M. (2022). Data-driven modelling of joint debris flow release susceptibility and connectivity. Earth Surf Process Landf. https://doi.org/10.1002/esp.5421

Stingl, V., & Mair, V. (2005). Einführung in die Geologie Südtirols:[aus Anlass des 32. *Internationalen Geologischen Kongresses im Sommer 2004 in Florenz]. Autonome Provinz Bozen-Südtirol*, Amt f. Geologie u. Baustoffprüfung.

Stoffel, M., Wyżga, B., & Marston, R. A. (2016). Floods in mountain environments: A synthesis. *Geomorphology*, *272*, 1–9. https://doi.org/10.1016/j.geomorph.2016.07.008

Surian, N., Righini, M., Lucía, A., Nardi, L., Amponsah, W., Benvenuti, M., Borga, M., Cavalli, M., Comiti, F., Marchi, L., Rinaldi, M., & Viero, A. (2016). Channel response to extreme floods: Insights on controlling factors from six mountain rivers in northern Apennines, Italy. *Geomorphology*, *272*, 78–91. https://doi.org/10.1016/j.geomorph.2016.02.002

Tischendorf, L., & Fahrig, L. (2000). How should we measure landscape connectivity? *Landscape Ecology*, *15*(7), 633–641. https://doi.org/10.1023/A:1008177324187

Wainwright, J., Turnbull, L., Ibrahim, T. G., Lexartza-Artza, I., Thornton, S. F., & Brazier, R. E. (2011). Linking environmental régimes, space and time: Interpretations of structural and functional connectivity. *Geomorphology*, *126*(3-4), 387–404. https://doi.org/10.1016/j.geomorph.2010.07.027

Walling, D. E., & Zhang, Y. (2004). Predicting slope-channel connectivity: A national-scale approach. In V. Golosov,

V. Belyaev, & D. E. Walling (Eds.), *Sediment Transfer Through the Fluvial System ICCE* (pp. 107–114). IAHS.

Wohl, E., Brierley, G., Cadol, D., Coulthard, T. J., Covino, T., Fryirs, K. A., Grant, G., Hilton, R. G., Lane, S. N., Magilligan, F. J., Meitzen, K. M., Passalacqua, P., Poeppl, R. E., Rathburn, S. L., & Sklar, L. S. (2019). Connectivity as an emergent property of geomorphic systems. *Earth Surface Processes and Landforms*, *44*(1), 4–26. https://doi.org/10.1002/esp.4434